SACLANTCEN MEMORANDUM
serial no.: SM-352

SACLANT UNDERSEA RESEARCH CENTRE MEMORANDUM

ACCURACY OF SYNTHETIC APERTURE SONAR MICRONAVIGATION USING A DISPLACED PHASE CENTRE ANTENNA

M. Pinto, S. Fioravanti, E. Bovio

February, 1999

Report no. changed (Mar 2006): SM-352-UU

SACLANT Undersea Research Centre
Viale San Bartolomeo 400
19138 San Bartolomeo (SP), Italy

tel: +39-0187-5271
fax: +39-0187-524.600

e-mail: library@saclantc.nato.int

NORTH ATLANTIC TREATY ORGANIZATION

Report no. changed (Mar 2006): SM-352-UU

Accuracy of synthetic aperture sonar micronavigation using a displaced phase centre antenna

M. Pinto, S. Fioravanti, E. Bovio

The content of this document pertains to work performed under Project 031-6 of the SACLANTCEN Programme of Work. The document has been approved for release by The Director, SACLANTCEN.

Jan L. Spoelstra
Director

intentionally blank page

Accuracy of synthetic aperture sonar micronavigation using a displaced phase centre antenna

M. Pinto, S. Fioravanti, E. Bovio

Executive Summary:

Higher resolution sonars will be required to detect and more importantly to classify mines, which are undetectable by existing sonars, for reasons of shape, material, size or location. Synthetic aperture sonar (SAS) will increase the sonar cross-range resolution by several orders of magnitude while maintaining or increasing the area search rate and thus contribute to an enhancement of mine hunting performance, in particular in shallow water, where smaller mines are more effective. The side scan configuration of SAS makes it well suited to remotely operated underwater vehicles, such as those forseen for covert survey and reconnaissance operations.

SAS performance is limited by the precision with which the motion errors of the platform can be estimated. The terminology of "micronavigation" is used to describe this very specific requirement for sub-wavelength short-term relative positioning. The aim of this work is to quantify the theoretical performance of data-driven micronavigation based on the displaced phase centre antenna (DPCA) concept. The unique feature of DPCA, of great pratical significance, is that it does not require the presence of seafloor features as it exploits the spatial coherence properties of seafloor reverberation.

intentionally blank page

Report no. changed (Mar 2006): SM-352-UU

Accuracy of synthetic aperture sonar micronavigation using a displaced phase centre antenna

M. Pinto, S. Fioravanti, E. Bovio

Abstract:

This work evaluates the accuracy of multi-element synthetic aperture sonar (SAS) micronavigation based on the concept of displaced phase centre antenna (DPCA).

The Cramér-Rao lower bound (CRLB) for the joint estimation of the ping-to-ping, translational and rotational displacement in the slant range plane (referred to as sway and yaw) is established. The CRLB on sway is shown to be proportional to the half-wavelength at the centre frequency $\lambda_0/2$ and that on yaw to $\lambda_0/(L-2D)$, the angular resolution of the DPCA (where L is the length of the physical reception aperture and $D \leq L/2$ the along-track, ping-to-ping displacement). Both CRLBs are also inversely proportional to the square root of an effective signal-to-noise ratio ρ_{eff} which is the product of the physical reverberation-to-noise ratio ρ by the number K of independent elements in the DPCA and the number BT of independent temporal samples used in the estimation (where B is the bandwidth and T the duration of the temporal estimation window).

The accuracy required on the sway and yaw to achieve a given SAS beampattern specification, determined by the expected loss ΔG in the SAS array gain, is computed as a function of the number P of pings in the SAS. Higher accuracy is required when P increases to counter the accumulation of errors during the integration of the elementary ping-to-ping estimates: the standard deviation must decrease like $P^{-1/2}$ for the sway and $P^{-3/2}$ for the yaw.

For given ΔG, the ρ_{eff} required to achieve a given gain Q in cross-range resolution (defined as the ratio of the resolution of the physical reception aperture to that of the SAS) is computed as a function of $\alpha = L/2D \geq 1$, the along-track SAS spatial sampling factor. It is shown that there exists a value of α which is optimal in the sense that it allows maximum Q for given ρ_{eff}.

The CRLBs are extended to include the effect of residual calibration errors of the physical reception array. It is shown that these errors set a lower bound on the achievable micronavigation accuracy even for infinite ρ_{eff}. The accuracy with which the physical array has to be calibrated to achieve a given SAS performance is computed as a function of the relevant SAS parameters.

Contents

1

Micronavigation using a displaced phase centre antenna

1.1 Multi-element SAS

The basic principle of synthetic aperture is well known from SAR (Synthetic Aperture Radar). However a SAR nearly always uses a single transducer for both transmission and reception. This design is not suited to high resolution sonar applications because it leads to unacceptably slow area search rates. A suitable design is to operate with a linear array of $N \geq 1$ receiving elements. This allows the spatial sampling, hence the area mapping rate, to be increased by a factor of N.

More precisely, consider a receiving aperture of N elements spaced at d, of total length $L = Nd$. At a given ping p, this has the same beam pattern as an Equivalent Real Array (ERA), at frequency $2f$, of N elements spaced at $d/2$. In far field conditions (which can be achieved after appropriate wavefront curvature corrections) the elements can be assumed located at the phase centres $C_{np} = (T_p + R_{np})/2$ where T_p (resp. R_{np}) is the position of the phase centre of the transmitter (resp. the position of the centre of element n) at ping p (Fig. 1). The ERA associated with the SAS consists of P sub-arrays, $\mathrm{ERA}_1, \mathrm{ERA}_2, ..., \mathrm{ERA}_P$, where ERA_{p+1} is displaced along-track by $D = Nd/2$ with respect to ERA_p. This ERA has a total of NP elements spaced at $d/2$ so that its total length is $PNd/2 = PL/2$, its angular resolution λ/PL and its grating lobes are spaced at λ/d. These grating lobes can be suppressed by increasing the spatial sampling of the physical reception aperture ($d < \lambda/2$) or, more cost-effectively, sufficiently reduced by placement in the far sidelobes of the transmission pattern. It is common practice in SAR to place these grating lobes between the first and second transmission sidelobe which leads to $d \leq L_t/2$, where L_t is the length of the transmitter.

1.2 Displaced phase centre antenna

The basic idea of a displaced phase centre antenna (DPCA) is to cancel the along-track, ping-to-ping displacement of the sonar platform by synthesis of an effective displacement, in the opposite direction, of a subset of receiving elements. This is achieved by operating at $D = Md/2$ with $M < N$ so that there are $K = N - M$

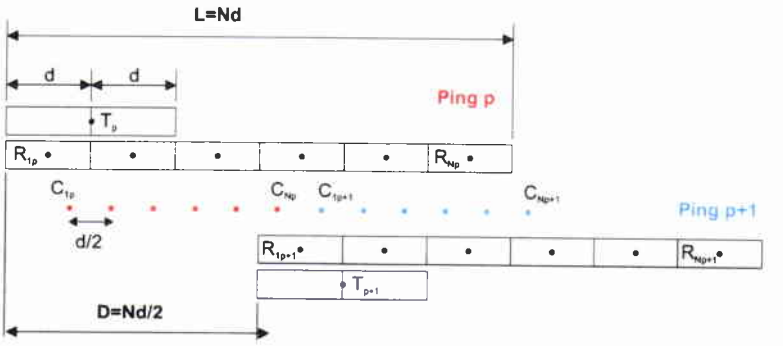

Figure 1 *Spatial sampling of a multi-element synthetic aperture sonar*

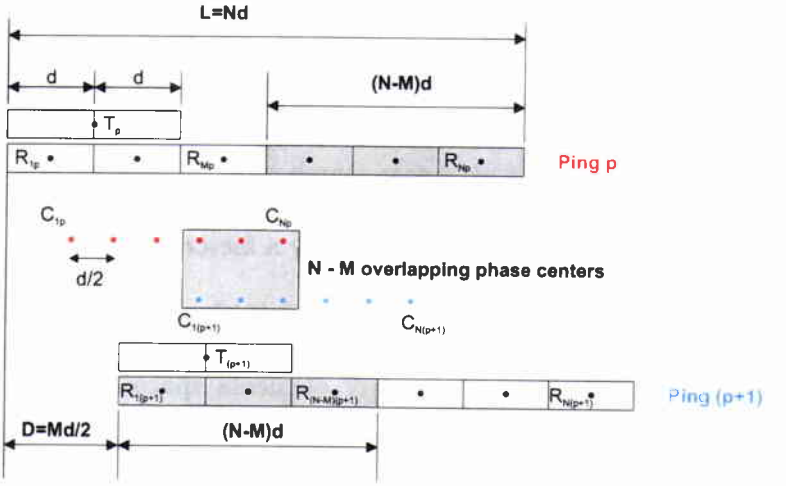

Figure 2 *Displaced phase centre antenna*

phase centres which overlap from ping to ping (see Fig. 2). The K corresponding receivers can be viewed as the K elements of a DPCA. In the absence of cross-track motion errors, the same waveform is transmitted and received twice from the K overlapped phase centres, so that the same echoes will be received at the two positions of the DPCA, with the same propagation delay, regardless of the spatial distribution of the elementary scatterers (Fig. 3). This argument assumes that noise has been disregarded and that scatterer geometry and the propagation medium have not changed.

DPCA is known in airborne radar, where it is used for detecting slowly moving targets in clutter, and also in sonar, where it forms the basis of correlation logs. There has been a revival of interest for this alternative to Doppler logs and the subject has recently been revisited theoretically by Doisy [1] who derived the accuracy of translational displacement estimates for volumetric arrays, as well as for attitude-stabilized planar arrays.

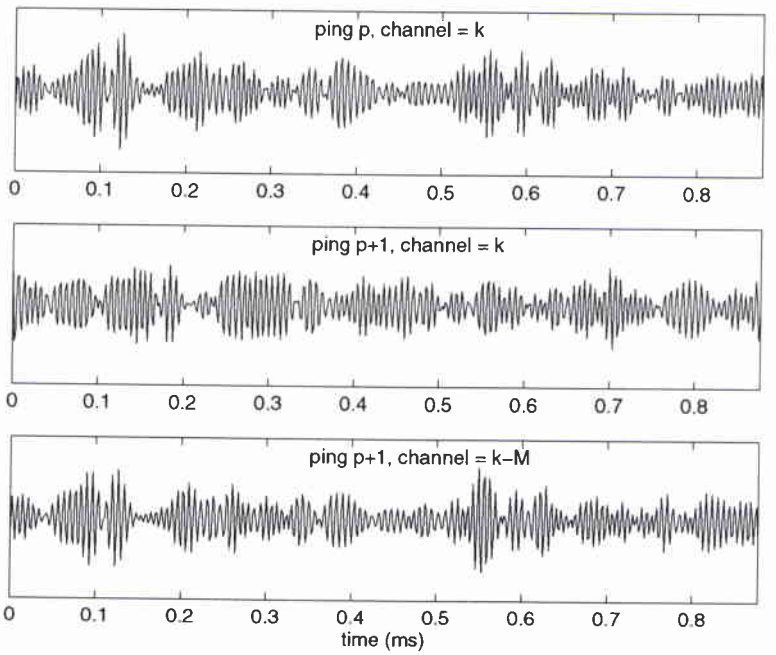

Figure 3 *Experimental (116-180 KHz) reverberation time series of overlapped phase centres (provided by DERA, UK).*

The application to SAS micronavigation is also far from new [2]. SAS micronavigation exploits a generalized form of the waveform invariance principle which can be explained intuitively as follows [3]. In the presence of cross-track motion errors, the two phase centres will no longer overlap but form a (synthetic) interferometric base (Fig. 4). The change in round-trip travel time to each scatterer will be determined by the projection of the baseline in the radial direction to the scatterer. If the angular spread of this direction within a given sonar resolution cell, or a set of resolution cells within a given time window, remains small compared to the angular resolution of the interferometric base, then the changes in travel time will be the same for all the scatterers in the resolution cell. For this time window, the two received signals will therefore be nearly identical in shape but received at slightly different delays after transmission. This difference provides an estimate of the line-of-sight motion error.

The loss in coherence which results from an excessive angular spread is known as *baseline decorrelation* in the remote sensing community where its effect on the precision of height estimation using interferometric sonar has been studied in some detail. Both problems are similar, as micronavigation exploits a synthetic along-track interferometer. When $K \geq 2$, a vector of time delays can be estimated and used to estimate both the translational and rotational ping-to-ping displacements in the slant-range plane. These will be referred to here as sway and yaw (Fig. 4).

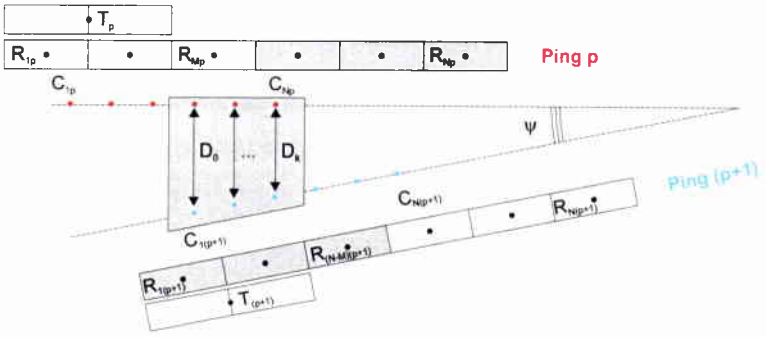

Figure 4 *Micronavigation with a displaced phase centre antenna*

By integrating the $P-1$ displacement estimates across the P pings in the SAS, the projection of the distorted synthetic array in the slant range plane can be reconstructed and subsequently beamformed (after suppression of one out of two of the redundant phase centres). The aim of this work is to study the residual accumulated error of the process and the limits imposed on the achievable SAS performance.

2

Cramér-Rao lower bounds on DPCA micronavigation

2.1 Cramér-Rao theorem

The scope of the Cramér-Rao Lower Bound (CRLB) is well known in signal theory [4]. The main features can be summarized as follows.

Let X be an observation distributed over a probability space Ω with probability distribution function:

$$p(X;\beta) \tag{1}$$

depending on a vector of parameters $\beta = (\beta_1, ..., \beta_q)$. Then for all bias-free estimator $\hat{\beta}(X)$ of β, covariance matrix V satisfies

$$V - F^{-1} \geq 0 \tag{2}$$

where F is the Fisher information matrix (FIM) of order q. The matrix F can be expressed as

$$F(k,l) = -\left\langle \frac{\partial^2 \mathcal{L}}{\partial\beta_k\beta_l} \right\rangle \tag{3}$$

where $\mathcal{L} = \mathrm{Log}\, p(X;\beta)$ is the log-likelihood and $\langle \cdot \rangle$ is the expectation operator.

2.2 Computation of the CRLBs for sway and yaw

Let $\{X_1(t), X_1'(t), X_2(t), X_2'(t), ..., X_K(t), X_K'(t)\}$ be the K pairs of signals received by the elements of the DPCA at two adjacent pings. We will assume that, over a small enough time window T, these signals can be expressed as:

$$X_k(t) = S_k(t) + N_k(t) \quad (4)$$
$$X'_k(t) = S_k(t - D_k) + N'_k(t) \quad (5)$$

where the noise signals N_k and N'_k are mutually independent and independent of the reverberation signals S_k. Furthermore the S_k are assumed independent from each other. This will obtain as long as two adjacent elements are separated by more than the spatial correlation length of the backscatter. It results from the Van-Cittert Zernike theorem, which states that, for statistically homogeneous reverberation, the spatial correlation function is the Fourier transform of the power transmission beam pattern [1] and that this correlation length is equal to the effective transmitter length L_t. The parameter K can be expressed as

$$K \simeq \frac{L - 2D}{L_t} \quad (6)$$

Reverberation and noise will be assumed to be Gaussian random processes with a flat power spectral density in the signal bandwidth. The reverberation to noise ratio will be denoted by $\rho = \langle S^2 \rangle / \langle N^2 \rangle$, where the noise has three different physical origins:

1. additive noise in the medium or in the receiver
2. baseline decorrelation (see previous chapter)
3. temporal decorrelation due to changes in the medium or the scattering geometry from ping to ping.

In far field conditions (which can be recovered in near field after the appropriate wavefront curvature corrections), the K components of the delay vector depend on two parameters

$$D_k(\gamma, \psi) = \frac{2\gamma}{c} + \psi \frac{2d_k}{c} \quad (7)$$

where

$$d_k = \left(k - 1 - \frac{K-1}{2}\right) \frac{d}{2} \quad (8)$$

is the abscissa of the phase centre of element k, with respect to the origin taken at the geometrical centre of the DPCA, γ is the sway and ψ the yaw (Fig. 4).

As (X_k, X'_k) and (X_l, X'_l) are independent for $k \neq l$, the log-likelihood relative to the two parameters (γ, ψ) can be expressed as a function of log-likelihood $\mathcal{L}_1(D)$ relative to the estimation of a single delay D as follows:

$$\mathcal{L}_K(\gamma, \psi) = \sum_{1 \leq k \leq K} \mathcal{L}_1(D_k(\gamma, \psi)) \tag{9}$$

The benefit of this formulation is that the different terms of the FIM of order 2 can be obtained as a function of K and the FIM of order 1 relative to the estimation of a single delay D, defined as $F_D = -\langle d^2\mathcal{L}_1/dD^2 \rangle$. The expression of $\sigma_D = 1/\sqrt{F_D}$ is a classical result of time delay estimation [5]:

$$\sigma_D = \frac{1}{\sqrt{8\pi^2}} \frac{1}{f_0} \frac{1}{\sqrt{BT}} \sqrt{\frac{2}{\rho} + \frac{1}{\rho^2}} \tag{10}$$

where B is the signal bandwidth.

One has

$$F_{\gamma,\gamma} = -\left\langle \frac{\partial^2 \mathcal{L}_K}{\partial \gamma^2} \right\rangle = -\frac{4}{c^2} K \left\langle \frac{d^2 \mathcal{L}_1}{dD^2} \right\rangle = \frac{4}{c^2} K F_D \tag{11}$$

and

$$F_{\psi,\psi} = -\left\langle \frac{\partial^2 \mathcal{L}_K}{\partial \psi^2} \right\rangle = -\frac{4}{c^2} \sum_{1 \leq k \leq K} d_k^2 \left\langle \frac{d^2 \mathcal{L}_1}{dD^2} \right\rangle = \frac{d^2}{c^2} \frac{K(K^2-1)}{12} F_D \tag{12}$$

As for the non-diagonal term

$$F_{\gamma,\psi} = -\left\langle \frac{\partial^2 \mathcal{L}_K}{\partial \gamma \partial \psi} \right\rangle = \frac{4}{c^2} F_D \sum_{1 \leq k \leq K} d_k = 0 \tag{13}$$

which shows that the estimations of γ and ψ are separable. The CRLBs can, after some elementary manipulations, be written as:

$$\sigma_{\gamma,0} = \frac{1}{\sqrt{8\pi^2}} \frac{\lambda_0}{2} \frac{1}{\sqrt{BT}} \frac{1}{\sqrt{K}} \sqrt{\frac{2}{\rho} + \frac{1}{\rho^2}} \tag{14}$$

$$\sigma_{\psi,0} = \sqrt{\frac{3}{2\pi^2}} \sqrt{\frac{K-1}{K+1}} \frac{\lambda_0}{(K-1)d} \frac{1}{\sqrt{BT}} \frac{1}{\sqrt{K}} \sqrt{\frac{2}{\rho} + \frac{1}{\rho^2}} \tag{15}$$

The physical interpretation of these formulas is straightforward:

The CRLB on γ is proportional to $\lambda_0/2$, the half-wavelength at the centre frequency. The CRLB on ψ is proportional to $\lambda_0/(K-1)d$, the angular resolution of the DPCA. Both CRLBs are inversely proportional to the square root of the number BT of independent temporal samples and to that of the number K of independent elements in the DPCA. They both decrease with the reverberation-to-noise ratio ρ, as $1/\rho$ for small ρ and $1/\sqrt{\rho}$ for large ρ. Finally a minimum of two elements is required to estimate the yaw (which is physically obvious).

The above expressions of the CRLBs show the importance of large bandwidth B for improved micronavigation accuracy. In addition there are benefits to operating with large K, as sway accuracy increases in proportion to $K^{1/2}$ and yaw accuracy increases in proportion to $K^{3/2}$, due to the combined effect of the increase (like K) in angular resolution of the DPCA and the increase (like $K^{1/2}$) of the number of independent spatial samples. It is seen from Eq. (6) that the way to increase K for given L is to reduce D, at the price of a reduced area mapping rate, or reduce L_t which leads to an increased number of elements in the physical aperture (since $d \leq L_t/2$).

2.3 *Effective signal-to-noise ratio*

Useful approximations of the CRLBs can be established as a function of two key SAS parameters which are

1. the SAS spatial sampling factor $\alpha = L/2D$
2. the effective signal-to-noise ratio $\rho_{\text{eff}} = KBT\rho$

One has

$$\frac{2\sigma_{\gamma,0}}{\lambda_0} = \frac{1}{2\pi} \frac{1}{\sqrt{\rho_{\text{eff}}}} \tag{16}$$

and

$$\frac{2D\sigma_{\psi,0}}{\lambda_0} = \frac{\sqrt{3}}{\pi} \frac{1}{\alpha - 1} \frac{1}{\sqrt{\rho_{\text{eff}}}} \tag{17}$$

where it has been assumed that $\rho \gg 1$, $K \gg 1$.

3

Accuracy requirements for sway and yaw

Let (O, x, y) be the slant range plane, with Ox along-track and Oy across-track, (x_p, y_p) the coordinates of the geometrical centre C_p of ERA_p, θ_p the angle between Oy and boresight to ERA_p.

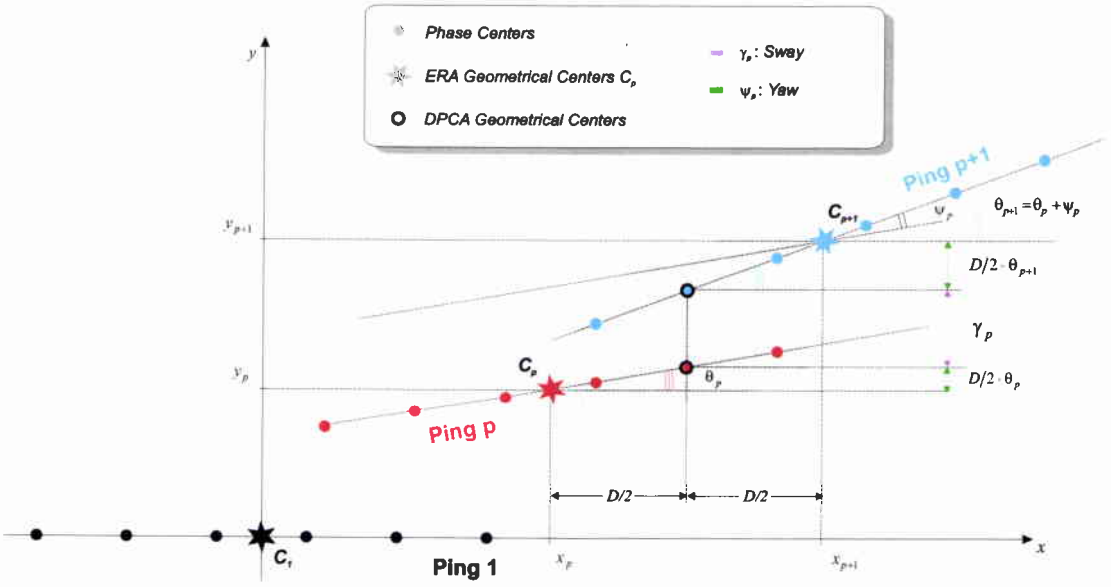

Figure 5 *2D geometry of motion*

In what follows we shall use the undistorted SAS as reference so that, without loss of generality, we assume $x_1 = y_1 = 0$ and $\theta_1 = 0$. The most important effect of micronavigation errors are cross-track position errors of C_p. One has, assuming small angles:

$$\begin{cases} x_{p+1} &= x_p + D \\ y_{p+1} &= y_p + \gamma_p + \frac{D}{2}\theta_p + \frac{D}{2}\theta_{p+1} \\ \theta_{p+1} &= \theta_p + \psi_p \end{cases} \tag{18}$$

where γ_p and ψ_p are the micronavigation errors on the sway and yaw between pings p and $p+1$. The quantity $y_{p+1} - y_p$ is seen to be the sum of three terms. The

first is the measurement error on the sway, whereas the last two result from errors in the pointing direction of the physical reception antenna at pings p and $p+1$. Indeed the spatial separation between the geometrical centre of the DPCA and that of the physical array is $D/2$, which leads to a difference in cross-track position of the associated equivalent phase centres of $D\theta_p/2$ and $D\theta_{p+1}/2$ (Fig. 5).

The SAS beampattern specification will be given in terms of the normalized expected gain of the SAS array factor:

$$G = \frac{1}{P^2}\left\langle \left| \sum_{p=1}^{P} \exp(j2k_0 y_p) \right|^2 \right\rangle \tag{19}$$

where $k_0 = 2\pi/\lambda_0$ is the wavenumber at the centre frequency. For small Gaussian errors, this can be also be expressed as :

$$G \simeq 1 - \frac{1}{P^2} \sum_{p=1}^{P} \sum_{q=1}^{p-1} \sigma_{p,q}^2 \tag{20}$$

where

$$\sigma_{p,q}^2 = \left\langle 2k_0 (y_p - y_q)^2 \right\rangle \tag{21}$$

Finally, we will also assume that γ_p and ψ_p are independent from each other and from ping to ping. Then the corresponding losses in SAS array gain are additive and can be studied separately.

3.1 Required sway accuracy

We assume that $\theta_p = 0$ for all p. Then

$$y_{p+1} = y_p + \gamma_p \tag{22}$$

Since

$$y_p - y_q = \sum_{l=q}^{p-1} \gamma_l \tag{23}$$

one has

$$\sigma_{p,q}^2 = (p-q)(2k_0\sigma_\gamma)^2 \tag{24}$$

where $\sigma_\gamma^2 = \langle\gamma^2\rangle$. Thus one obtains finally

$$G \simeq 1 - \frac{2\pi^2}{3}(P - \frac{1}{P})\left(\frac{2\sigma_\gamma}{\lambda_0}\right)^2 \simeq 1 - \frac{2\pi^2}{3}P\left(\frac{2\sigma_\gamma}{\lambda_0}\right)^2 \tag{25}$$

The required accuracy for sway can therefore be expressed as a function of the number P of pings in the SAS and the loss in normalized array gain $1-G$ as (Fig. 6):

$$\frac{2\sigma_\gamma}{\lambda_0} \leq \sqrt{\frac{3(1-G)}{2\pi^2 P}} \tag{26}$$

It is seen that, for given G, the standard deviation of the sway estimation is required to decrease like $P^{-1/2}$ to combat the accumulation of errors.

3.2 *Required yaw accuracy*

We assume $\gamma_p = 0$ for all p. Then

$$y_{p+1} = y_p + \frac{D}{2}(\theta_p + \theta_{p+1}) \tag{27}$$

where

$$\theta_p = \sum_{m=1}^{p-1} \psi_m \tag{28}$$

After algebraic manipulations (Annex 1), G can be expressed as a function of P and $2D\sigma_\psi/\lambda_0$, where $\sigma_\psi^2 = \langle\psi^2\rangle$:

$$G \simeq 1 - \frac{\pi^2}{30}(P - \frac{1}{P})(4P^2 - 5P - 1)\left(\frac{2D\sigma_\psi}{\lambda_0}\right)^2 \tag{29}$$

$$\simeq 1 - \frac{\pi^2}{15}P(4P^2 - 5P - 1)\left(\frac{2D\sigma_\psi}{\lambda_0}\right)^2 \tag{30}$$

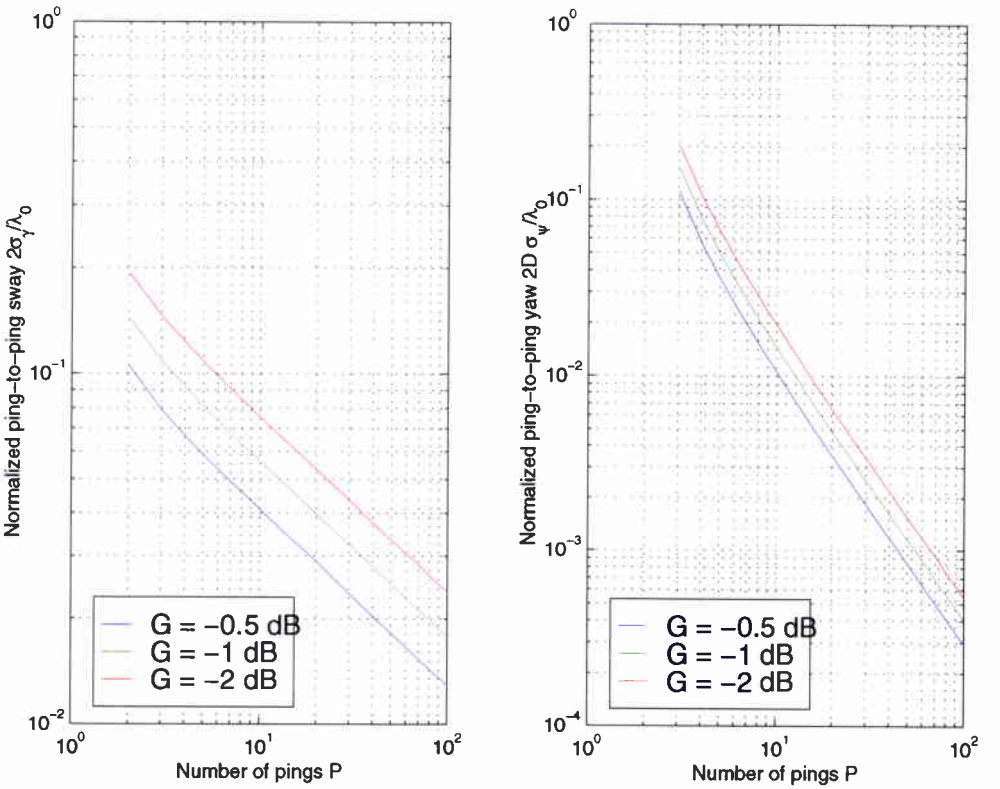

Figure 6 *Accuracy requirements for sway and yaw estimation*

The required accuracy for the yaw can therefore be expressed as a function of the number P of pings in the SAS and the loss in normalized array gain $1 - G$ as:

$$\frac{2D\sigma_\psi}{\lambda_0} \leq \sqrt{\frac{30(1-G)}{\pi^2 P(4P^2 - 5P - 1)}} \tag{31}$$

For large enough P, the accuracy requirement is seen to vary in proportion to $P^{-3/2}$ instead of $P^{-1/2}$ (Fig. 6).

4

Required effective signal-to-noise ratio

By combining the expressions of the CRLBs given by Eq. (14) with the requirements as described by Eq. (26) and Eq. (31) it is possible to determine the effective signal-to-noise ratio ρ_{eff} to achieve a given SAS performance.

4.1 Requirements for sway

From Eq. (16) and Eq. (26), one obtains

$$\rho_{\text{eff}} \geq \frac{P - 1/P}{6(1-G)} \simeq \frac{P}{6(1-G)} \tag{32}$$

To facilitate the interpretation, it is useful to introduce the parameter $Q = 1 + (P - 1)/\alpha$ which corresponds to the gain in cross-range resolution of the SAS over the physical reception aperture. The inequality then becomes

$$\rho_{\text{eff}} \geq \frac{\alpha(Q-1)+1}{6(1-G)} \tag{33}$$

which is plotted on Fig. 7 for $G = -1$ dB and for various values of α.

4.2 Requirements for yaw

Likewise, by combining Eq. (17) and Eq. (31), one obtains:

$$\rho_{\text{eff}} \geq \frac{P(4P^2 - 5P - 1)}{10(1-G)(\alpha-1)^2} \tag{34}$$

and

$$\rho_{\text{eff}} \geq \frac{(\alpha(Q-1)+1)(4(\alpha(Q-1)+1)^2 - 5(\alpha(Q-1)+1) - 1)}{10(1-G)(\alpha-1)^2} \tag{35}$$

which is plotted on Fig. 7. The requirements for accurate yaw estimation are seen to be higher, by several orders of magnitude, than those for sway. Meeting these requirements will be challenging, in particular when attempting to maximize simultaneously the area mapping rate, which requires operating at values of α as close to 1 as possible.

The right hand side of Eq. (35) behaves approximately like $\alpha^3/(\alpha-1)^2$ which decreases from $+\infty$ to a minimum attained for $\alpha = 3$ and then increases monotonically to ∞. The minimum corresponds to the best compromise between the conflicting requirements of increasing α, to increase the resolution of the DPCA and the accuracy of the yaw estimation and decreasing α, to reduce the total number of pings P for given Q and limit the accumulation of errors. Therefore $\alpha = 3$ is the optimal oversampling factor in the sense that it allows the largest Q for given ρ_{eff} (or equivalently smallest ρ_{eff} for given Q). The price to pay is a mapping rate reduced by a factor of $1/\alpha$. There is therefore a tradeoff between resolution gain and area mapping rate which characterizes DPCA-micronavigated SAS.

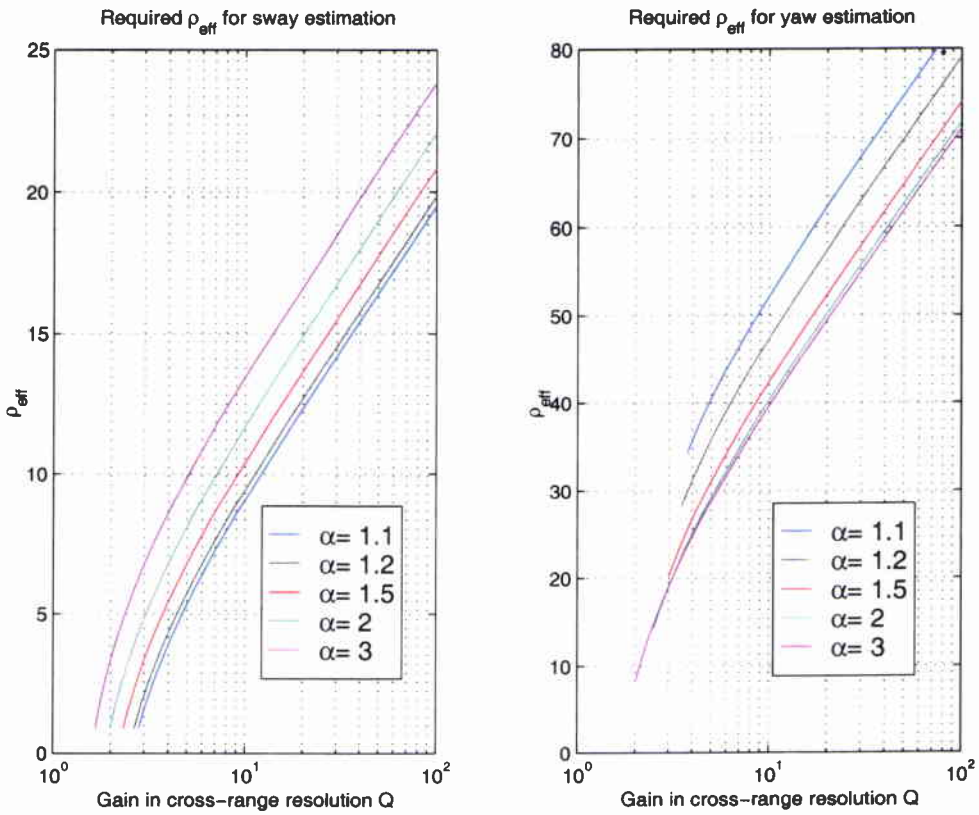

Figure 7 *ρ_{eff} requirements for sway and yaw estimation*

5

Cramér-Rao bounds in presence of physical calibration errors

Interchangeability of the receiver channels is a basic condition of the success of the DPCA technique. Therefore micronavigation accuracy will be affected also by residual calibration errors of the physical aperture.
The generalized CRLBs, including the effect of calibration errors, can be computed by use of an extended formalism discussed by [4]

5.1 Extended Cramér-Rao theorem

In this formalism the vector β is no longer deterministic but becomes a random vector with *a priori* distribution $p_0(\beta)$. Then the Fisher information matrix can be written as

$$F = F_d + F_a \tag{36}$$

where F_d can be expressed, as previously, as a function of the log-likelihood

$$\mathcal{L}_d = \mathrm{Log}\, p(X;\beta) \tag{37}$$

as

$$F_d(k,l) = -\left\langle \frac{\partial^2 \mathcal{L}_d}{\partial\beta_k \beta_l} \right\rangle \tag{38}$$

and F_a can be expressed as a function of

$$\mathcal{L}_a = \mathrm{Log}\, p_0(\beta) \tag{39}$$

as

$$F_a(k,l) = -\left\langle \frac{\partial^2 \mathcal{L}_a}{\partial \beta_k \beta_l} \right\rangle \tag{40}$$

The terms relative to F_a vanish for deterministic parameters. If the vector β is now written as

$$\beta = (\beta_d, \beta_a) \tag{41}$$

where β_d represents the set of deterministic parameters to be estimated (e.g. the sway and yaw) and β_a the set of random parameters (the residual calibration errors) the Fisher information matrix can be written as a bloc matrix

$$\begin{pmatrix} F(\beta_d, \beta_d) & F(\beta_d, \beta_a) \\ F(\beta_a, \beta_d) & F(\beta_a, \beta_a) \end{pmatrix} \tag{42}$$

One has

$$F(\beta_d, \beta_d) = F_d(\beta_d, \beta_d) \tag{43}$$

and

$$F(\beta_a, \beta_a) = F_d(\beta_a, \beta_a) + F_a(\beta_a, \beta_a) \tag{44}$$

When β_a is assumed Gaussian of covariance Φ one has furthermore

$$F_a(\beta_a, \beta_a) = \Phi^{-1} \tag{45}$$

Thus the final expression of the Fisher information matrix becomes

$$\begin{pmatrix} F_d(\beta_d, \beta_d) & F_d(\beta_d, \beta_a) \\ F_d(\beta_a, \beta_d) & F_d(\beta_a, \beta_a) + \Phi^{-1} \end{pmatrix} \tag{46}$$

5.2 Computation of the extended CRLBs

The time-delay vector of Eq. (7) becomes

$$D_k = \frac{2\gamma}{c} + \psi\frac{2d_k}{c} + \epsilon_k \tag{47}$$

where ϵ_k is the timing error representative of the mismatch between the two receiving channels which form element k of the DPCA. The phase errors $\Phi_k = 2\pi f_0 \epsilon_k$ will be assumed independent, Gaussian with zero-mean and standard deviation σ_Φ.

One starts from

$$\mathcal{L}_d(\gamma, \psi, \epsilon) = \sum_{1 \le k \le K} \mathcal{L}_1(D_k(\gamma, \psi, \epsilon_k)) \tag{48}$$

since the K channels of the DPCA are assumed independent. One then has

$$F = \begin{pmatrix} \frac{4}{c^2}KF_D & 0 & \frac{2}{c}F_D & \frac{2}{c}F_D & \dots & \frac{2}{c}F_D \\ 0 & \frac{K(K^2-1)}{12}\frac{d^2}{c^2}F_D & \frac{2d_1}{c}F_D & \frac{2d_2}{c}F_D & \dots & \frac{2d_K}{c}F_D \\ \frac{2}{c}F_D & \frac{2d_1}{c}F_D & F_D + F_\epsilon & 0 & \dots & 0 \\ \frac{2}{c}F_D & \frac{2d_2}{c}F_D & 0 & F_D + F_\epsilon & \dots & 0 \\ \vdots & \vdots & \vdots & \vdots & \vdots & \vdots \\ \frac{2}{c}F_D & \frac{2d_K}{c}F_D & 0 & 0 & \dots & F_D + F_\epsilon \end{pmatrix} \tag{49}$$

where F_D is, as previously, the FIM of order 1 relative to the estimation of a single deterministic delay D and $F_\epsilon = (2\pi f_0/\sigma_\Phi)^2$. The extended CRLBs are obtained by inverting this generalized FIM of order $K+2$. One obtains

$$\sigma_\gamma^2 = \sigma_{\gamma,0}^2 + \sigma_{\gamma,cal}^2 \tag{50}$$

$$\sigma_\psi^2 = \sigma_{\psi,0}^2 + \sigma_{\psi,cal}^2 \tag{51}$$

with

$$\sigma_{\gamma,cal} = \frac{1}{2\pi}\frac{1}{\sqrt{K}}\frac{\lambda_0}{2}\sigma_\Phi \tag{52}$$

$$\sigma_{\psi,cal} = \frac{\sqrt{3}}{\pi}\sqrt{\frac{K-1}{K+1}}\frac{1}{\sqrt{K}}\frac{\lambda_0}{(K-1)d}\sigma_\Phi \tag{53}$$

where $\sigma_{\gamma,0}$ and $\sigma_{\psi,0}$ are the Cramér-Rao bounds in the absence of calibration errors, as given by Eq. (14) and Eq. (15). Thus that calibration errors set a lower bound on the achievable sway and yaw accuracy even for infinite ρ_{eff}. To facilitate comparisons with Eq. (16) and Eq. (17), these expressions can be rewritten as:

$$\frac{2\sigma_{\gamma,cal}}{\lambda_0} = \frac{1}{2\pi}\frac{1}{\sqrt{K}}\sigma_\Phi \tag{54}$$

and

$$\frac{2D\sigma_{\psi,cal}}{\lambda_0} = \frac{\sqrt{3}}{\pi}\frac{1}{\alpha-1}\frac{1}{\sqrt{K}}\sigma_\Phi \tag{55}$$

5.3 *Calibration accuracy requirements*

The required calibration accuracy can be derived very simply from the above expressions by noting the similarity of Eq. (16) and Eq. (17) with Eq. (54) and Eq. (55). Both set of equations can be made identical by introducing

$$\rho_{\text{eff,cal}} = \frac{K}{\sigma_\Phi^2} \tag{56}$$

Then Fig. 7 can be used directly to specify the required calibration accuracy, with $\rho_{\text{eff,cal}}$ in place of ρ_{eff}.

6

Conclusion

The accuracy of synthetic aperture sonar (SAS) micronavigation based on the displaced phase centre antenna technique (DPCA) has been studied theoretically. The two most important parameters which govern micronavigated SAS performance are:

1. the spatial oversampling factor α (defined as $L/2D$ where L is the length of the physical reception array and D the ping-to-ping displacement)
2. the effective signal-to-noise ratio ρ_{eff}, defined as the product of the reverberation-to-noise ratio ρ, by the number K of independent elements in the DPCA and the number BT of independent temporal samples used in the estimation (B is the bandwidth and T the length of the correlation window).

Spatial oversampling $\alpha > 1$ is a fundamental constraint of DPCA micronavigation. The micronavigation accuracy increases with α as long as $1 < \alpha \leq 3$ whereas the achievable area mapping rate A decreases with α. Thus there is a tradeoff between the cross-range resolution of a SAS and the area mapping rate. Different applications may require different tradeoffs.

Whereas modest values of ρ_{eff} are required for sway, values higher by several orders of magnitude are required for yaw. This will be facilitated by the use of sonar designs which incorporate recent advances in imaging technology, such as arrays with the high temporal and spatial sampling required to support very wide bandwiths (leading to BT values ranging from 100 to 1000 or more) and broad transmission sectors (leading to values of K ranging from 10 to 100) without aliasing. The feasibility of obtaining such high values in realistic experimental situations warrants further investigation.

The most important single environmental parameter is the reverberation to noise ρ. In addition to noise in the medium or in the receiver, which can be countered by increasing the energy in the transmitted waveform, the sources of noise are baseline decorrelation and temporal decorrelation. The in-depth understanding of the underlying physical processes should be an integral part of any research into SAS.

Baseline decorrelation depends on the amplitude of the platform motion errors, measured in wavelengths, as well as on the bottom type and its local topography which

determine the line of sight direction. It can be minimized by a a stabler platform design, reducing the operating frequency (although this make it more difficult to achieve a given resolution) or improved signal processing (such as an additional stage of beamforming with the DPCA, to reduce the angular spread of the line of sight direction). Temporal decorrelation relates to ping-to-ping changes in the medium, such as those due to time-varying multipath and water column effects.

Instrumentation could be considered as a means of further increasing micronavigation performance enhancement. High quality attitude rate sensors achieve a level of accuracy sufficient, in principle, for yaw estimation. Micronavigation techniques which fuse yaw information provided by instrumentation with sway information provided by the sonar would increase by one order of magnitude or more the resolution gain achievable by SAS. However, whereas the sonar directly measures the platform motion in the slant range plane, strap-down sensors measure motion in a frame linked to the platform which must subsequently be projected in the slant range plane. This poses no problem in principle, but does requires knowledge of the local grazing angle which remains unknown when imaging is performed with a conventional linear array. Bathymetric imaging, such as that provided by an interferometric SAS, may be a solution which warrants further investigation.

Acknowledgements

The authors are grateful to A. Bellettini for the many improvements to the original document.

References

[1] Doisy, Y., General motion estimation from correlation sonar. *IEEE Journal on Oceanic Engineering*, **23**, 1998: 127–140.

[2] Sammelmann, G., Fernandez J.E. *et al.*, High frequency, low frequency synthetic aperture sonar. *Naval Research Reviews*, **49**, 1997: 3–8.

[3] Pinto, M.A. *et al.*, Autofocusing a synthetic aperture sonar using the temporal and spatial coherence of seafloor reverberation. In: Pace, N.G. *et al.*, High Frequency Acoustics in Shallow Water. (SACLANTCEN CP-45) pp. 417–424. [ISBN 88-900194-1-7]

[4] Kopp, L., Thubert, D., Bornes de Cramer-Rao en traitement d'antenne. *Traitement du signal*, **3**, 1986: 111–125 and **4**, 1987: 57–71.

[5] Quazi, A.H., An overview on the time delay estimate in active and passive systems for target localization. *IEEE Transations on Acoustics, Speech, and Signal Processing*, **29**, 1981: 527–533.

Annex 1

From Eq. (27) we can write

$$\begin{aligned} y_{p+1} &= y_p + D\sum_{m=1}^{p-1}\psi_m + \frac{D}{2}\psi_p \\ &= D\sum_{l=1}^{p}\sum_{m=1}^{l-1}\psi_m + \frac{D}{2}\sum_{l=1}^{p}\psi_l \\ &= D\sum_{l=1}^{p}\left(p-l+\frac{1}{2}\right)\psi_l, \end{aligned} \tag{A-1}$$

whence

$$y_p = D\sum_{l=1}^{p-1}\left(p-l-\frac{1}{2}\right)\psi_l. \tag{A-2}$$

Since the ψ_l are independent from each other, one has

$$\left\langle (y_p - y_q)^2 \right\rangle = D^2(p-q)^2\sum_{l=1}^{q-1}\left\langle \psi_l^2 \right\rangle + D^2\sum_{l=q}^{p-1}\left(p-l-\frac{1}{2}\right)^2\left\langle \psi_l^2 \right\rangle. \tag{A-3}$$

When the error $\sigma_\psi = \sqrt{\left\langle \psi_p^2 \right\rangle}$ on the ping-to-ping sway is the same for every ping the previous equation becomes

$$\left\langle (y_p - y_q)^2 \right\rangle = D^2\sigma_\psi^2\left[(p-q)^2(q-1) + \sum_{l=q}^{p-1}\left(p-l-\frac{1}{2}\right)^2\right]. \tag{A-4}$$

We have then

$$\begin{aligned} \sum_{p=1}^{P}\sum_{q=1}^{p-1}\left\langle (y_p - y_q)^2 \right\rangle &= D^2\sigma_\psi^2\sum_{p=1}^{P}\frac{(p-1)p(2p-1)(2p-3)}{24} \\ &= D^2\sigma_\psi^2\frac{(P-1)P(P+1)(4P^2-5P-1)}{120}. \end{aligned} \tag{A-5}$$

The normalized expected gain of the SAS is finally

$$
\begin{aligned}
G &= 1 - \frac{4k_0^2}{P^2} \sum_{p=1}^{P} \sum_{q=1}^{p-1} \left\langle (y_p - y_q)^2 \right\rangle \\
&= 1 - \frac{\pi^2}{30}(P - \frac{1}{P})(4P^2 - 5P - 1) \left(\frac{2D\sigma_\psi}{\lambda_0} \right)^2 \qquad \text{(A-6)}
\end{aligned}
$$

Report no. changed (Mar 2006): SM-352-UU

Document Data Sheet

Security Classification		Project No.
UNCLASSIFIED		031-6
Document Serial No.	**Date of Issue**	**Total Pages**
SM-352	February 1999	31 pp.

Author(s)

Pinto, M., Fioravanti, S., Bovio, E.

Title

Accuracy of synthetic aperture sonar micronavigation using a displaced phase centre antenna

Abstract

This work evaluates the accuracy of multi-element synthetic aperture sonar (SAS) micronavigation based on e concept of displaced phase centre antenna (DPCA).

The Cramer-Rao lower bound (CRLB) for the joint estimation of the ping-to-ping, translational and rotational displacement in the slant range plane (referred to as sway and yaw) is established. The CRLB on sway is shown to be proportional to the half-wavelength at the centre frequency $\lambda_0/2$, and that on yaw to $\lambda_0/L_r - 2D$), the angular resolution of the DPCA (where L_r is the length of the physical reception aperture and $D \geq L_r/2$ the along track, ping-to-ping displacement). Both CRLBs are also inversely proportional to the square root of an effective signal-to-noise ratio ρ_{eff} which is the product of the reverberation-to-noise ratio ρ by the number K of independent elements in the DPCA and the number BT of independent temporal samples in the estimation (where B is the bandwidth and T the duration of the correlation window).

The accuracy required on the sway and yaw to achieve a given SAS beampattern specification, determined by the expected loss ΔG in the SAS array gain, is computed as a function of the number P of pings in the SAS. Higher accuracy is then required when P increases to counter the accumulation of errors during the integration of elementary ping-to-ping estimates: the standard deviation must decrease like $P^{-1/2}$ for the sway and $P^{-3/2}$ for the yaw.

For a given ΔG, the ρ_{eff} required to achieve a given gain Q in cross-range resolution over that of the physical reception aperture is computed as a function of $\alpha = L_r/2D \geq 1$, the along-track SAS spatial sampling factor. It is shown that there exists a value of α which is optimal in the sense that it requires minimal ρ_{eff} for given Q (or maximum Q for given ρ_{eff}).

The CRLBs are extended to include the effect of residual calibration errors of the physical reception array. It is shown that these errors set a lower bound on the achievable micronavigation accuracy even for infinite ρ_{eff}. The accuracy with which the physical array has to be calibrated to achieve a given SAS performance is computed as a function of the relevant SAS parameters.

Keywords

Issuing Organization

North Atlantic Treaty Organization
SACLANT Undersea Research Centre
Viale San Bartolomeo 400, 19138 La Spezia, Italy

[From N. America: SACLANTCEN (New York) APO AE 09613]

Tel: +39 0187 527 361
Fax:+39 0187 524 600

E-mail: library@saclantc.nato.int

Report no. changed (Mar 2006): SM-352-UU

Initial Distribution for Unclassified SM-352

Scientific Committee of National Representatives

SCNR Belgium	1
SCNR Canada	1
SCNR Denmark	1
SCNR Germany	1
SCNR Greece	1
SCNR Italy	1
SCNR Netherlands	1
SCNR Norway	1
SCNR Portugal	1
SCNR Spain	1
SCNR Turkey	1
SCNR UK	1
SCNR USA	2
SECGEN Rep. SCNR	1
NAMILCOM Rep. SCNR	1

National Liaison Officers

NLO Canada	1
NLO Denmark	1
NLO Germany	1
NLO Italy	1
NLO Netherlands	1
NLO Spain	1
NLO UK	3
NLO USA	4
Sub-total	29
SACLANTCEN library	21
Total	50